HHS Public Access

Author manuscript

Free Radic Res. Author manuscript; available in PMC 2019 February 01.

Published in final edited form as:

Free Radic Res. 2018 February ; 52(2): 288–303. doi:10.1080/10715762.2018.1431626.

Hydrogen sulfide increases glutathione biosynthesis, and glucose uptake and utilization in C_2C_{12} mouse myotubes

Rajesh Parsanathan and **Sushil K. Jain***

Department of Pediatrics, Louisiana State University Health Sciences Center, Shreveport, Louisiana 71130, United States

Abstract

Diabetic patients have lower blood concentrations of hydrogen sulfide (H_2S), L-cysteine (LC), and glutathione (GSH). Using C_2C_{12} mouse myotubes as a model, this study investigates the hypothesis that the beneficial effects of LC supplementation are mediated by upregulation of the H_2S status under diabetic conditions. Results show that exogenous administration of sodium hydrosulfide (NaHS, 10 or 20 μM; 6 hours), a H_2S donor, significantly ($p<0.05$) upregulates the gene expression of cystathionine-γ-lyase (CSE), LC transporter (Slc7a11/xCT), and the genes involved in GSH biosynthesis. Additionally, it reduces homocysteine (HCys), reactive oxygen species (ROS) production, and enhances cellular LC, H_2S, and glucose uptake and utilization in myoblasts. The use of CSE siRNA to induce deficient endogenous H_2S production causes an increase in H_2O_2, ROS, HCys levels, and downregulation of GSH biosynthesis pathway enzymes. In additional, CSE knockdown downregulates glucose transporter type 4 (GLUT4) and gene expression of its key transcription factors, and reduces glucose uptake in C_2C_{12} myotubes. CSE knockdown cells showed specific increases in the protein S-glutathionylation of LC transporter and GLUT4 along with increased total protein S-glutathionylation. Taken together, evidence from this study provides molecular insights into the importance of the CSE/H_2S system in maintaining the cellular glutathione and glucose homeostasis in C_2C_{12} myotubes.

Graphical abstract

*Corresponding author address: Sushil K. Jain, PhD, Department of Pediatrics, Louisiana State University Health Sciences Center, 1501 Kings Highway, Shreveport, Louisiana 71130 USA, Tel: +1-318-675-6086, FAX: +1-318-675-6059, sjain@lsuhsc.edu.

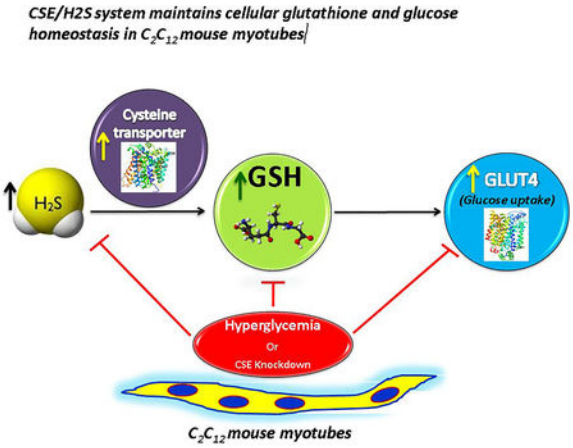

Keywords

Cystathionine-γ-lyase (CSE); hydrogen sulfide (H_2S); glutathione; GLUT4; Slc7a11/xCT; C_2C_{12}; glucose homeostasis

Introduction

Diabetes is associated with lower blood concentrations of L-cysteine (LC), glutathione (GSH), and hydrogen sulfide (H_2S) [1–13]. LC undergoes enzymatic breakdown to produce H_2S, a gasotransmitter that regulates glucose and lipid homeostasis. Gut bacteria are reported to engender significant amounts of H_2S [14]. In addition, human diets rich in organosulfur compounds, such as garlic, onions, leeks, and chives has been reported to contribute to the H_2S pool and to exert a beneficial influence on the metabolic state and hypertension [15]. H_2S production occurs in a defined tissue milieu and sub-cellular spaces through the action of specific enzymes. Similarly to nitric oxide (NO) and carbon monoxide (CO), H_2S has been shown to be a gaseous transmitter that plays an important role in normal physiological processes as well as in the process/progression of several diseases. Thus far, four main enzymatic contributors of endogenous H_2S have been identified: cystathionine-γ-lyase (CSE), cystathionine β-synthase (CBS), and cysteine aminotransferase (CAT) in conjunction with 3-mercaptopyruvate sulfurtransferase (3-MPST) [16–19]. These enzymes occur widely in mammalian cells and tissues and produce H_2S, which in turn plays multiple roles in regulating cardiovascular function, inflammation, insulin resistance, and glucose metabolism [20].

Human studies have shown that decreased levels of H_2S are associated with high glucose/insulin resistance/T1D/T2D conditions [1–13,21–23]. *In vitro* and *in vivo* studies suggest a potential role for reduced H_2S levels in the impaired glucose homeostasis found in diabetes [24,25]. Skeletal muscle is a major site for the maintenance of glucose homeostasis in the human body. However, neither the precise biological effect of either endogenous or exogenous H_2S on myotubes, nor its contribution to antioxidant and glucose homeostasis, is clear. This study examined the functional relationship between H_2S and GSH biosynthesis in the regulation of cyst(e)ine transporter (Slc7a11/xCT) as an upstream thiol component of

GSH, a potent antioxidant defense response as a downstream cascade, and of insulin-sensitive glucose transporter type 4 (GLUT4), a master regulator of glucose homeostasis, in a myotube cell model. Results from this study suggest that H_2S enhances GSH biosynthesis and promotes glucose uptake and utilization.

Materials and methods

Materials

All chemicals, unless specified, were purchased from Sigma. Antibodies against glutathione [D8] (ab19534), GCLC (ab53179), GCLM [EPR6667] (ab126704), glutathione synthetase [EPR6562] (ab124811), glutathione reductase (ab16801), xCT or Slc7a11 (ab37185), PPARα (ab24509), PPARγ (ab19481), PGC1α (ab54481), Vitamin D receptor (ab3508), and β-actin HRP (ab49900) were purchased from Abcam. The anti-CTH (WH0001491M) and anti-GLUT4 (G4048) were purchased from Sigma Aldrich. Goat anti- mouse HRP (170–6516) was purchased from Biorad and the goat anti-rabbit HRP (12–348) from Millipore. Pierce™ protein A/G agarose was purchased from Thermo Scientific.

Cell culture

Mouse C_2C_{12} myoblasts (American Type Culture Collection no. CRL-1772) were cultured at 37°C in an atmosphere of 5% CO_2 in growth medium (GM) consisting of Dulbecco's modified Eagle's medium (DMEM) supplemented with 10% fetal bovine serum and antibiotics (penicillin, streptomycin). Differentiation of myoblasts into myotubes was induced when the cells had achieved 90 to 95% confluence by switching the medium from GM to differentiation medium (DM) consisting of DMEM supplemented with 2% horse serum (5 days). Reduction of serum allowed cell-to-cell fusion and formation of myotubes. The cells were examined each day to evaluate the degree of differentiation, which was determined as the percentage of nuclei present in the multinucleated myotubes under a phase contrast microscope.

NaHS doses and treatment

Differentiated myotubes were exposed to 0, 10, or 20 μM NaHS for 6 h in serum and Phenol Red-free medium. We used NaHS (sodium hydrosulfide) as a donor for H_2S. When NaHS is dissolved in water, HS^- is released and forms H_2S with H^+ [26,27]. This provides a solution of H_2S with a better-defined concentration in terms of both accuracy and reproducibility when compared to a solution obtained by bubbling H_2S gas through water. It was estimated that the systemic concentration of H_2S ranges from 20–300μM [17], and the presence of this low amount of H_2S might be responsible for its physiological antioxidative properties. Hence, to better mimic the physiological level of H_2S, C_2C_{12} myotubes were incubated with a H_2S donor, NaHS (10 and 20μM).

CSE RNAi, high glucose and NaHS treatment

CSE siRNA and control siRNA were purchased from Santa Cruz Biotechnology (Santa Cruz, CA). CTH (CSE) siRNA for mouse (sc-142618) is a pool of 2 different siRNA duplexes: Sense: CUGAAUUUGGACUGAAGAUtt; Antisense: AUCUUCAGUCCAAAUUCAGtt; Sense: CGAUGUUGUCAUGGGUUUAtt; Antisense:

UAAACCCAUGACAACAUCGtt. The double-stranded control siRNA-A sequence r(UUCUCCGAACGUGUCACGU)d(TT) (sc- 37007) does not match other current sequences. All sequences are provided in $5' \rightarrow 3'$ orientation. Cells were transfected with either 50 or 100 nM siRNA complex as follows. Briefly, 3 or 6 μL 10 μM specified siRNA diluted in 100 μL transfection media (Santa Cruz) was mixed with 3 or 6 μL Lipofectamine™ 2000 transfection reagent (Invitrogen, Carlsbad, CA), respectively, and incubated for 30 min at room temperature to form siRNA complexes. The siRNA medium was formed by addition of 500 μL transfection media to the siRNA complexes to yield a concentration of 50 and 100 nM specified siRNA. Cells were incubated with siRNA medium for 4 h at 37°C followed by incubation with fresh complete media for the next 24 h. After the transfection procedure, cells were treated with serum and Phenol Red-free medium for 6 h, similar to the NaHS treatment. Stock solutions for high glucose (HG) were made in sterilized water. Cells were treated with HG (25 mM) for 24h. The glucose concentration of 25 mM was similar to that used in other studies [28]. Patient data suggest that glucose levels can sometimes become elevated to 30 mM [29]. High glucose exposed and CSE deficient cells were treated with 20 μM NaHS for 6 h in serum and Phenol Red-free medium [30]. Cell viability was determined in all treatments to rule out cell death. Cells were used to perform intracellular ROS, H_2S, GSH, LC, and homocysteine analyses, quantitative PCR, Western blotting, and immunoprecipitation analysis.

Cell viability assay

Cell viability was determined using the Alamar Blue reduction bioassay. This method is based upon Alamar Blue dye reduction by live cells. Briefly, cells were plated into 96 well plates after treatment per the above-described protocols, AlamarBlue® Cell Viability Reagent (DAL1100, ThermoFisher Scientific) was added, and the cells were incubated at 37°C in the dark for 4 h. Absorbance was read at 590 nm using a plate reader. Data are expressed as a percentage of viable cells.

In situ cellular hydrogen sulfide measurement

Free sulfide was measured in cells using a specific fluorescent probe, sulfide fluor-7 acet oxymethyl ester [SF_7-AM] (748110, ALDRICH). SF_7-AM is a fluorogenic, or 'caged' rhodamine 110 derivative used for the detection of hydrogen sulfide (H_2S). Upon exposure to H_2S, the azide functional groups are reduced to primary amines, restoring the fluorescence of the 'caged' fluorophore. A fluorescence intensity increase of 20× is observed following 1 h of SF_7- AM exposure to H_2S. This activation of SF_7-AM has been shown to detect H_2S levels as low as 500 nM *in vitro* [31]. After appropriate treatment conditions, C_2C_{12} myotubes were incubated with 2.5 μM SF_7-AM in Phenol Red-free medium for 30 min and rinsed with SF_7-AM free medium. Fluorescence was measured at 495 nm/519 nm. The fluorescent intensity at a certain time point (F0) divided by the fluorescent intensity at the zero-time point (Fi) is denoted as F0/Fi. Results are presented as the fold change of F0/Fi over that of the control group.

Intracellular ROS production

Intracellular reactive oxygen species (ROS) levels were measured in treated cells using the oxidant-sensitive probe 2′,7′dichlorofluorescein diacetate [H_2DCFDA] (D6883 SIGMA);

the probe was added at a concentration of 20 μM and the cells were incubated at 37°C for 30 min in the dark. As H_2DCFDA diffuses passively through the cellular membrane, intracellular esterase activity removes the diacetate group and the resulting H_2DCF reacts with any ROS in the cell and fluoresces [32]. After incubation with the dye the cells were washed once with PBS and the intensity of DCF fluorescence was measured at filter settings of 485 nm excitation and 528 nm emission, respectively, using a multidetection microplate reader (Synergy HT, BIOTEK). The change in intracellular ROS levels was plotted as mean fluorescence intensity (MFI).

Determination of peroxide levels

The levels of hydrogen peroxide were determined in cells using a modification of the method described by Barja (1999) [33]. Briefly, after treatment cells were washed twice with phosphate-buffered saline (PBS) and then incubated at 37°C with a PBS solution containing 0.1 mm homovanilic acid and 6 U mL^{-1} horseradish peroxidase for 5 min. The incubation was stopped with 1 mL of cold 2 M glycine buffer containing 50 mM EDTA and 2.2 M NaOH. The fluorescence of the supernatant was measured using 312 nm excitation and 420 nm emission [34]. The levels of peroxides were calculated using a standard curve of H_2O_2 dilutions and were expressed as μM of H_2O_2.

Glucose utilization and uptake assays

The glucose utilization level was determined by subtracting glucose values at the end of the experiments (leftover glucose) from the 0 h glucose level. All assays were done in duplicate at each time point. A Bayer Contour Next EZ Glucose Meter (Bayer HealthCare LLC, Mishawaka, IN, USA) was used for the glucose utilization assay. The glucose utilization values were expressed in mmol/L. The glucose uptake assay was performed using 6-NBDG (Invitrogen), a fluorescent analog of 2-deoxyglucose, following the method of Jung *et al.* [35]. Briefly, after treatment, cells were incubated with serum-free low glucose medium containing 6- NBDG (20 μM) for 30 min. After the incubation, cells were washed with PBS and then lysed with 70 μL of PBS containing 1% Triton X-100 and kept at dark for 10 min. Then 30 μL dimethyl sulfoxide was added to each sample and homogenized by pipetting up and down, and the plate was read immediately using a microplate reader at excitation/ emission wavelengths of 466/540 nm. Results were expressed as relative fluorescence units (RFU).

Quantitative real-time reverse transcription polymerase chain reaction analysis

Total RNA extraction from C_2C_{12} myotubes was performed using TRIzol reagent (Invitrogen). The concentration and quality of the extracted RNA were determined on a NanoDrop spectrophotometer (Thermo Scientific). RNA (1 μg) from each sample was reverse transcribed according to the manufacturer's instructions using a High Capacity RNA-To-cDNA kit (Applied Biosystems) to synthesize cDNA. QPCR was performed using the Applied Biosystems™ TaqMan™ Gene Expression Assays with primer/probe sets (Supplementary Table 1). The relative amount of mRNA was calculated using the relative quantification (ΔΔCT) method. The relative amount of each mRNA was normalized to housekeeping gene Gapdh. According to MIQE guidelines, the technical replicates (n=3) and biological replicates (n=4) was done in all our experiments. Data were analyzed by the

comparative CT method and the fold change was calculated by the $2^{-\Delta\Delta CT}$ method [36] using a 7900HT Real Time PCR system and software (Applied Biosystems). The results were expressed as relative quantification (RQ).

Preparation of whole cell extracts

For whole cell extraction, after treatment the cells were washed twice with ice-cold PBS and lysed in RIPA buffer (50 mM Tris pH 8, 150 mM NaCl, 1% NP-40, 0.5% deoxycholic acid, and 0.1% SDS) supplemented with protease and phosphatase inhibitors (1 mM PMSF, 5 μg/mL leupeptin, 2 μg/mL aprotinin, 1 mM EDTA, 10 mM NaF, and 1 mM NaVO4). Lysates were then centrifuged for 10 min at 10,000 × *g* at 4°C. Supernatants were collected and the protein concentrations were determined using a BCA assay kit (Pierce/Thermo Scientific, Rockford, IL) for Western blot analysis and HPLC assay.

Western blot analysis

Equal amounts (20 μg) of proteins were separated on 10 % SDS-PAGE and transferred to a polyvinyl difluoride (PVDF) membrane. Membranes were blocked at room temperature for 2 h in a blocking buffer containing 1% BSA to prevent non-specific binding and then incubated with an appropriate primary antibody at 4°C overnight. The membranes were washed in TBS-T (50 mmol/L Tris–HCl, pH 7.6, 150 mmol/L NaCl, 0.1 % Tween 20) for 30 min and incubated with the appropriate HRP-conjugated secondary antibody (1:5000 dilution) for 2 h at room temperature. The protein bands were detected using ECL detection reagents (Thermo Scientific) and exposed on blue X-ray film (Phenix Research Products, Candler, NC). The technical replicates (n=2) and biological replicates (n=4) was done in all our immunoblot experiments. Western blot scans were analyzed using ImageJ software (developed by Wayne Rasband, National Institutes of Health, Bethesda, MD; available at http://rsb.info.nih.gov/ij/index.html). Densitometric analyses of Western blots were normalized with respect to β-actin (Ratio).

GSH, L-Cysteine, and homocysteine analysis

GSH analysis was carried out following the modified method of Pfeiffer *et al.* [37]. Cell lysates were used to determine GSH levels using high-performance liquid chromatography (Waters, Milford, MA) complexed to a 2475 fluorescent detector with 385 nm emission and 515 nm excitation wavelengths as described earlier [7]. Briefly, equal protein concentrated cell lysate sample (20μg) was made-up with 100μl of PBS and incubated with 10μl of Tris(2- carboxyethyl)phosphine (TCEP 100g /L of PBS, pH 7.4) for 30 min at room temperature to reduce the disulfides and release protein-bound thiols. Deproteinization was achieved by the addition of 90μl of 100 g/L trichloroacetic acid containing 1 mM EDTA. Precipitated proteins were removed by centrifugation at 15000g for 3 min, and 50μl of supernatant was mixed with 185μl of derivatization solution containing 125μl of 0.125M borate buffer containing 4 mM EDTA (pH 9.5), 50μl of 1 g/L SBD-F (7-Fluorobenzofurazan-4-sulfonic acid ammonium salt) in the borate-EDTA buffer and 10μl of NaOH (1.55M). The sample was then incubated for 60min at 60°C in the dark. Standards and blank were prepared in the same way of the samples. After derivatization, the samples, standards and blank were cooled on ice and protected from light until injection onto the column. Mobile phase: Acetic acid-acetate buffer with methanol (0.1M AAA buffer pH 5.5,

containing 30ml/L methanol); flow rate 0.7ml/minute. Typically, 10μl of samples, standards and blank was injected onto the column (C_{18}). The fluorescence intensities were measured with excitation at 385 nm and emission at 515 nm. Data are expressed as nmol/mg protein.

Immunoprecipitation and protein S-glutathionylation analysis

Total protein S-glutathionylation was quantified with an anti-GSH antibody and normalized with β-actin under non-denaturing conditions. Briefly, equal amounts (20 μg) of lysates were separated under non-denaturing conditions and the proteins transferred to a PVDF membrane. They were probed with anti-GSH antibody overnight then incubated with the appropriate HRP-conjugated secondary antibody (1:5000 dilution) for 2 h at room temperature. The protein bands were detected using ECL detection reagents (Thermo Scientific) and exposed on blue X-ray film (Phenix Research Products, Candler, NC). Densitometric analyses of total protein S-glutathionylated blots were normalized with respect to β-actin (Ratio).

After appropriate treatments, equal amounts (1 mg) of proteins prepared under non-denaturing conditions from cells were incubated first with protein A/G agarose to remove nonspecific binding to protein A/G agarose. Anti-GSH antibody (10 μg) was then added, and the mixture was incubated at 4°C overnight. The antigen-antibody complexes were pulled down by incubation with protein A/G agarose at 4°C for 2 h. After 3 washes with phosphate-buffered saline, the bound proteins were released by the addition of 50 μL non-reducing SDS sample buffer and heating at 96°C for 3 min. After a brief centrifugation, 20 μL of each supernatant was separated and immune blotted with anti-xCT and anti-GLUT4 and quantified. Detected bands were normalized with control and expressed as % control.

Sequence alignments and molecular modeling

Comparison of the amino acid sequences of Slc7a11/xCT human (Q9UPY9 in the UniProtKB database), mouse (Q9WTR6), and rat (D4ADU2), and a similar comparison of sequences of Slc2a4/GLUT4 human (P14672), mouse (P14142), and rat (P19357) indicated that the localization of cysteine residues is conserved in all species. Amino acid sequences were aligned with default parameters and checked for transmembrane annotation to rule out the transmembrane cysteine residues. The structures of Slc7a11 (xCT) and Slc2a4 (GLUT4) were not available; therefore, three-dimensional models of the mouse Slc7a11 and Slc2a4 were created based on the previously published crystallographic 2.21 Å structure of the *Escherichia coli* arginine/agmatine antiporter (Protein Data Bank code 5J4I) [38] and the crystallographic

1.5 Å structure of human GLUT3 (4ZW9) [39], respectively. Considering the wide family of solute carriers implicated in human disease, GLUT4 and GLUT3 have significant sequence and structural homology with same substrate specificity and kinetic behaviors to many transporters and its biological function in this class [40]. Further, GLUT3 have highest similar positions of key sequences compared to other members (GLUT2 and GLUT1) of the same class. SWISS- MODEL workspace was used to generate models for mouse Slc7a11 (Q9WTR6) and Slc2a4 (P14142). The SWISS-MODEL template library (SMTL version 2016-11-09, PDB release 2016-11-05) was searched with Blast [41] and HHBlits [42] for

evolutionarily related structures matching the target sequences. Homology modeling for mouse Slc7a11 and Slc2a4 was carried out using a default parameter setup [43–45].

Statistical analysis

The data were subjected to one-way analysis of variance (ANOVA) followed by Student-Newman-Keul's (SNK) test to assess the significance between control and experimental groups. Wilcoxon's rank sum test (for independent samples) was used to compare two groups. The data are expressed as mean ± standard error of mean (SEM) and considered statistically significance at $p<0.05$. All analyses were performed using GraphPad Prism version 6.00 for Windows (GraphPad Software, La Jolla, California, USA).

Results

Treatment with NaHS (a H_2S donor) and cell viability in C_2C_{12} mouse myotubes

NaHS at a concentration of 10 or 20 μM and CSE siRNA treated (50 nM or 100 nM) myotubes cell viability was not affected (Figure 1(A, B)). As shown in Figure 1 (C), compared to those in the control group, fold changes in fluorescence intensity increased significantly and dose-dependently after NaHS treatment (10 or 20 μM), indicating that exogenous administration of a hydrogen sulfide donor increases cellular H_2S levels. CSE is the one of the principle enzymes involved in H_2S biosynthesis. Moreover, CSE knockdown caused a dose-dependent decline in fluorescence intensity for H_2S (Figure 1 (D)).

NaHS treatment significantly ($p<0.05$) reduced ROS production in myotubes at the 20 μM dose, whereas treatment with the 10 μM dose did not cause statistically significant results (Figure 1 (E)). CSE knockdown myotubes showed significant higher ROS production compared to controls, but there was no difference between results with 50 nM or 100 nM CSEsiRNA (Figure 1 (F)). The same trend was observed in peroxide levels in both cells and culture supernatant (Supplementary Figure 3(A,B)). This suggests that the endogenous H_2S produced by CSE is essential for its antioxidative activity.

CSE/H_2S signaling up-regulates CSE, Slc7a11 (xCT), and GSH biosynthetic pathways

Cystine is transported into cells by the highly specific amino-acid antiporter system x_c^- (xCT) [46]. Slc7a11 (xCT) and CSE were upregulated by H_2S in a dose-dependent manner (Figure 2 (A,B) left panel). To further verify whether the xCT and CSE upregulation were due to actions of the CSE/H_2S system, myotubes were transfected with an siRNA duplex targeting CSE mRNA, and the protein expression levels were assessed using immunoblotting. CSE expression was successfully suppressed as shown by the decrease of gene expression in the siRNA- transfected groups as compared with that in the scrambled-siRNA negative control (Supplementary Figure 2(A)). Surprisingly, we did not see any downregulation in the xCT of the CSE knockdown cells (Supplementary Figure 2(B)), but protein was declined in a dose- dependent manner (Figure 2 (A,B) right panel). Taken together, these observations suggest that inhibition of CSE gene expression that affects the xCT system post-translationally may not have an effect on transcriptional control in myotubes.

Glutathione helps protect cells from free radical damage by acting as an antioxidant. Glutamate cysteine ligase (GCL) is a heterodimeric holoenzyme composed of two protein subunits (GCLC and GCLM). GCL conjugates glutamate with a cysteine residue to form the dipeptide γ-glutamylcysteine (γ-GC), which is the rate-limiting step of *de novo* glutathione biosynthesis. Subsequently, glycine is added to the C-terminal of γ-glutamylcysteine via the enzyme glutathione synthetase (GSS), which catalyses the final step of GSH synthesis. GR is essential to recycling the GSSG back to its reduced form (GSH). There was a significant upregulation in the expression levels of these antioxidative mRNA (Supplementary Figure 1(C,D,E)) and proteins observed in the NaHS exposed group (Figure 2 (E,F,I,K) left panel). However, significant downregulation in the expression levels was seen in the case of CSE knockdown cells (Figure 2 (G,H,J,L) right panel). This suggests that H_2S might regulate cellular redox by altering levels of small molecule oxidant scavengers.

H_2S increases cellular glutathione pool and decreases homocysteine

L-Cysteine is the rate-limiting substrate for cellular GSH biosynthesis, typically present in its oxidized form cystine in the extracellular space. The sulfhydryl group (SH) of cysteine serves as a proton donor and is responsible for its biological activity. The increased expression of xCT in the presence of H_2S and decreased expression of xCT in CSE knockdown cells alters cellular LC levels because xCT is the key transporter providing cells with cysteine. The level of cysteine mirrors that of its transporter; the cellular cysteine levels significantly increased upon NaHS exposure (Figure 3(A)), whereas CSE deficient cells showed a dose-dependent decline in cysteine levels (Figure 3(B)).

The total glutathione concentration was increased significantly in a concentration- dependent manner following treatment with exogenous H_2S, as compared to CSE knockdown cells compared with the scrambled-siRNA-treated cells (Figure 3(A,B)). These results indicate that the loss of CSE decreases cellular glutathione concentration, thus predisposing the cells to oxidative stress and increased ROS production.

The trans-sulfuration enzymes CBS and CSE are critical in that they not only metabolize homocysteine irreversibly into cysteine, but also generate H_2S and dictate the anti-oxidant capacity of the cellular milieu [47]. Figure 3 (A, B), shows that cellular homocysteine marginally but significant decreased following NaHS exposure, whereas CSE knockdown cells showed increased levels of the same compared to that of controls. This may be due to altered expression of CSE and xCT in our study. Taken together, these data provide evidence that CSE possesses antioxidant activity, which suggests that the cytoprotective effects of the CSE/H_2S system may occur through glutathione homeostasis.

CSE/H_2S system upregulates GLUT4 and its transcription factors

GLUT4 and redox signaling play pivotal roles in cellular glucose homeostasis [48]. Figure 4 (A–J) total protein levels of GLUT4 and its key transcription factors VDR, PPARα, PPARγ, and PGC1α in myotubes exposed to NaHS and CSE knockdown cells. NaHS upregulated the protein levels of GLUT4 and its transcription factors significantly (Figure 4 (A,C,D,G,H)); at the mRNA level, VDR and PPARγ showed significant increases, but the remaining genes (Supplementary Figure 1(F–J)), were not altered at the transcription level.

As shown in Figure 4 (B,E,F,I,J), exposure to CSE knockdown cells caused a significant decrease in the protein levels of GLUT4 and its transcription factor. Surprisingly, mRNA levels of GLUT4 and VDR were downregulated in the 100 nM CSE-siRNA group compared to those in the scrambled control siRNA group (Supplementary Figure 2(F–J)). NaHS treated cells showed a significant dose-dependent increase in glucose uptake and utilization (Figure 5 (A,C)). Together, these observations suggest that inhibition of CSE gene expression by siRNA affects the GLUT4 and glucose metabolism.

Deficiency of H_2S/CSE knockdown increases total protein S-glutathionylation

Protein S-glutathionylation in protecting proteins from oxidative stress, in signal transduction and in the modulation of protein function [49], we investigated protein S-glutathionylation with immunoblotting using an anti-GSH antibody. Significantly increased total glutathionylated proteins were observed in CSE knockdown cells in comparison with those of the controls (Figure 6). In addition, a significant decrease of S-glutathionylation was detected in 20 μM NaHS treated cells. Protein glutathionylation is closely associated with oxidative stress [50]; this finding suggests that increased ROS in CSE knockdown cells may be the reason behind the elevated protein S-glutathionylation observed in our study.

CSE knockdown increases Slc7a11 (xCT) and Slc2a4 (GLUT4) glutathionylation

GSH and GSSG are known to be able to modify protein thiol groups by introducing disulfide bonds between the protein thiols and GSSG/GSH. Mouse xCT contains 6 cysteines (Figure 7(A)), all of which are highly conserved; mouse GLUT4 contains 4 cysteines (Figure 7(B)), of which 3 residues are highly conserved (C223, C361 and C363), while residue C430 is replaced by serine in human GLUT4. Since the structure of neither transporter was available, a model was generated based on the structure of the homologous templates of the arginine/agmatine antiporter (PDB ID: 5J4I) and solute carrier family 2, facilitated glucose transporter member 3 (PDB ID: 4ZW9), respectively. With respect to the amino acid sequence of human, mouse, and rat Slc7a11 and Slc2a4, the positions of the cysteine^{158} in xCT and cysteine^{223} in GLUT4 were marked between transmembrane III-IV in xCT and next to transmembrane VI in GLUT4, since these residues are not present in a transmembrane region that may be a potential target for S-glutathionylation. To examine whether direct S- glutathionylation occurring in xCT and GLUT4 was responsible for the observed functional alterations in cellular cysteine levels and glucose uptake, the following experiments were performed. First, S-glutathionylated proteins were precipitated from extracts of either NaHS treated or CSE knockdown cells by using an antibody directed against GSH under non-reducing conditions. As shown in Figure 7 (A,B), CSE knockdown caused an increase in S- glutathionylation in both xCT and GLUT4; in contrast, 10 μM NaHS had no significant effect on glutathionylation in xCT, nor did it influence S-glutathionylation in GLUT4, whereas 10 μM NaHS caused a marginal increase in xCT S-glutathionylation.

Exogenous NaHS (a H_2S donor) supplementation improves GSH and, glucose uptake in CSE KD and high glucose exposed myotubes

High glucose-induced significant downregulation of CSE (Figure 8(A)) and GLUT4 (Figure 8(G)) was observed in the present study. Exogenous H_2S may suppress the high glucose-

induced alteration in CSE and GLUT4 via GSH biosynthetic pathway by upregulating the key molecules such as SLC7A11, GCLC, GCLM (Figure 8(B–D)), leading to an increase in GSH, and glucose uptake (Figure 8(K,J)), preventing ROS generation (Figure 8(I)) and, there is not much alteration seen in CBS (Figure 8(E)) and 3−MPST levels (Figure 8(F)). H_2S levels in myotubes were also increased at the end of treatment (Figure (8H)). Exogenous H_2S treatment significantly improves CSE, SLC7A11, GCLC, GCLM, GLUT4 (Figure 9(A–D,G), and thus increases glucose uptake (Figure 9(J)). Further, reduced ROS (Figure 9(I)) and improved H_2S and GSH (Figure 9(H,K)) were observed in H_2S treated cells compared to CSE deficient cells. Surprising, we did not found much alteration in CBS and 3-MPST (Figure 9(E,F)) in CSE deficient cells.

Taken together, these observations suggest that inhibition of CSE gene expression (knockdown or high glucose) that affects the xCT system, GSH and glucose uptake at least in myotubes. However, significant alteration in other H_2S enzymes such as CBS and 3-MPST in HG as well as CSE deficient cells was not pronounced much in the case of myotube. This suggests that CSE principally regulate myotubes cellular redox by altering levels of H_2S in pathological conditions like diabetes mellitus.

Discussion

The glutathione-dependent system is one of the key pathways regulating cellular redox balance [51]. Cysteine is the rate-limiting substrate for cellular glutathione biosynthesis. Cyst(e)ine is transported into cells by the highly specific amino-acid antiporter system x_c^- [52]. Glutathione deficiency/inadequacy is often associated with impaired redox and has been implicated in the pathophysiology of various chronic diseases, such as diabetes [53]. This study shows that exogenous exposure to H_2S enhances CSE and Slc7a11 protein levels, whereas CSE knockdown (H_2S deficiency) cells showed the opposite. In addition, CSE deficiency reduces levels of the enzymes involved in GSH biosynthesis and cellular L-cysteine levels, and elevated homocysteine levels in myotubes. This suggested that endogenous H_2S plays a role in GSH biosynthesis.

GSH homeostasis is tightly controlled by GCLC, GCLM, GSS, and GR [54]. CSE deficiency reduced, but H_2S induced, the expression of all these genes in our study. Nrf2 is a master regulator of the antioxidant response and Keap1 acts as a negative regulator of Nrf2. It has been shown recently that NaHS S-sulfhydrated Keap1 at cysteine-151 induced Nrf2 dissociation from Keap1, enhanced Nrf2 nuclear translocation, and stimulated mRNA expression of Nrf2-targeted multiple downstream genes encoding for proteins that protect cells against oxidative stress, such as GCLC, GCLM, and GR [54–57]. GCLC, GCLM, and GR contain a common DNA regulatory cis-acting element, called ARE [antioxidant response element] (5’- TGACTnnnGC-3’), which is present in the promoter region of all of the antioxidant genes targeted by Nrf2. This suggests that upregulation of the genes involved in the antioxidant pathway in our study may be due to Keap1 Cys151-S-sulfhydration and nuclear translocation of Nrf2.

The main route for extracellular acquisition of LC is the transport of its disulfide form, cystine (CSSC), through the xCT(−) CSSG/$_L$-glutamate ($_L$-Glu) antiporter (SLC7A11)

system. Under conditions of elevated ROS, endogenous LC production is insufficient for GSH synthesis [58]. Furthermore, we observed that CSE deficiency is associated with significantly reduced intracellular GSH levels. This could be due to low endogenous H_2S levels in CSE knockdown cells, because supplementation with NaHS significantly increased GSH levels and attenuated cellular oxidative stress. The relatively low concentrations and considerably smaller size of H_2S compared with other low-molecular-weight thiols make it unlikely that it plays a quantitatively significant role in cellular antioxidant function via direct scavenging of ROS [59]. Additionally, while we found increased GR levels in H_2S exposed cells, CSE deficient cells showed reduced levels of GR. Oxidized glutathione needs to be channeled into a chained recycling system involving GR-thioredoxin enzymes using NADPH as a consumable reductant [60]. Since H_2S is a strong reducing thiol, it may also act through the thioredoxin or NADPH systems to exert its antioxidative properties, as both the GSH and thioredoxin mechanisms are interconnected and thiol-based [61]. Although knowledge of the complete underlying mechanism responsible for how H_2S undergoes disulfide exchange with oxidized glutathione is inconclusive, our data, which show that the cells exposed to H_2S had higher GSH levels as compared with those of the non-treated control, may suggest that the glutathione recycling rate is enhanced. CSE/H_2S may also act on the NADPH/NADP-GSH/GSSG systemic balance to exert its antioxidative activity [62]. These data provide evidence that H_2S may regulate the cellular redox balance and protect cells from oxidative insults during disease-induced glutathione depletion.

Dysfunction of GLUT4 is implicated in insulin resistance/diabetes mellitus [63]. This study shows that GLUT4 gene expression is affected by the CSE/H_2S system, where CSE deficiency showed reduced GLUT4, but H_2S enhanced GLUT4 levels in myotubes. GLUT4-dependent glucose uptake and oxidation are essential functional processes, which supply energy to cells to allow execution of diverse functions [64]. The rate of glucose oxidation in a cell depends on the rate of entry of glucose into the cell. In this study, glucose uptake and utilization were adversely affected by CSE deficiency, while H_2S exposure increased the physiological processes of GLUT4. Previous studies reported that L-cysteine, the precursor for both GSH and H_2S, favors GLUT4 translocation towards the plasma membrane (PM) and enhances glucose uptake [12,21]. Consequently, we explored the possible mechanism behind the defective GLUT4 gene expression and translocation towards the PM. The levels of transcription factors involved in transcription as well as translocation of GLUT4 are affected in CSE knockdown cells, but H_2S has a positive effect over these factors in gene expression (VDR, PPARα,γ, and PGC-1α). This suggests that reduced expression of GLUT4, along with its transcription and translocation factors, may contribute to the overall impaired glucose uptake and utilization observed in this study.

Hydrogen sulfide (H_2S) has been found to play beneficial roles in the pathophysiology of several diseases, including diabetes, hypertension, atherosclerosis, and cardiac/renal ischemia–reperfusion injuries [65]. CSE, CBS, and 3-MPST, the main enzymes in the transsulfuration pathway, catalyze H_2S production in mammalian tissues. However, the distributions and precise roles of these enzymes in the myotubes/muscle have not yet been identified. We detected expression of all three enzymes (CSE, CBS, and 3-MPST) in the mouse myotubes. CSE expression was markedly reduced under experimental diabetic conditions (hyperglycemia), whereas expression of CBS and 3-MPST was unaffected and

those of CSE, GCLC, GCLM, and GLUT4 were ameliorated by NaHS treatment. In addition, NaHS enhances GCL gene expression, increases GSH content, and prevents ROS production, thereby escalating glucose uptake in myotubes. Similar to results seen in other studies, those in our study indicate that CSE reduction results in decreased H_2S formation [66]. Parallel studies using H_2S supplementation of CSE KD myotubes showed a similar trend, such as a hyperglycemia induced effect in myotubes, where NaHS brought back the effects caused by CSE deficiency. These findings suggest that CSE expression and H_2S production in mouse myotubes may regulate insulin signaling via the GSH pathway. A physiologic role for H_2S in regulating glucose homeostasis raises the possibility that pharmacologic enhancement of H_2S formation could be an adjuvant therapy to prevent diabetes associated complications.

Reactive cysteine residues play a significant role in redox sensing, acting as protein redox switches in response to cellular oxidation or nitrosation; physiologically, they are responsible for relevant modulatory effects on protein function. GSH and GSSG are known to be able to modify protein thiol groups by introducing disulfide bonds between protein thiols and GSSG/GSH. With respect to the importance of protein S-glutathionlylation in protecting proteins from oxidative stress, in signal transduction and in the modulation of protein function, we demonstrated here that the condition of CSE deficiency enhanced protein S-glutathionylation globally and that the same trend was reflected in the GLUT4 and cysteine transporter. Further studies are needed on site specific Slc2a4 and Slc7a11 cysteine post-translational modifications, such as the role of glutathionylation/sulfhydration in redox imbalance status, to help to elucidate the intrinsic activity characterization and translocation towards plasma membrane/membrane trafficking of those transporters. Moreover, previous studies have shown that protein S-glutathionylation is linked to oxidative stress [50]; this finding suggests that the increased cellular ROS observed under CSE deficient conditions may be the reason behind the elevated protein S- glutathionylation observed in our study. Future studies of other signaling molecules redox switches involvement in the dynamics of GLUT4 and SLC7A11 transporters may provide strong evidence to support this.

In conclusion, this study reports for the first time that H_2S upregulates GCL, GSS, and GR, increases cellular GSH, and decreases ROS levels in myotubes. Our results revealed dual roles for H_2S as (1) a stimulator of GSH-dependent antioxidant defense, and (2) a regulator of cysteine homeostasis through its transporter. In addition, H_2S enhances insulin-sensitive GLUT4/Slc2a4 independent of insulin and its metabolic action (glucose uptake) in C_2C_{12} myotubes (Figure 10). Hyperglycemia is a major risk factor for the development of cellular complications associated with diabetes. The understanding and validation of mechanistic insights by which H_2S supplementation improves glycemia should support the design of clinical intervention using novel molecules (containing sulfide and cysteine moieties) to improve glucose metabolism. This study suggests a potential role for H_2S donors as an adjuvant therapy in the treatment of metabolic complications in diabetes.

Supplementary Material

Refer to Web version on PubMed Central for supplementary material.

Acknowledgments

The authors acknowledge Ms. Morgan for critical proof reading and excellent editing of this manuscript.

Funding

This work was supported by grants from the National Institutes of Health/National Center for Complementary and Integrative Health [RO1 AT007442, 2013–16], and the Malcolm W. Feist Cardiovascular Research Fellowship and Endowed Chair in Diabetes, Center for Cardiovascular Diseases and Sciences (**CCDS**) from LSUHSC, Shreveport.

References

[1]. Jain SK. L-cysteine supplementation as an adjuvant therapy for type-2 diabetes. Can J Physiol Pharmacol 2012;90(8):1061–4. [PubMed: 22783875]

[2]. Jain SK, Bull R, Rains JL, Bass PF, Levine SN, Reddy S, McVie R, Bocchini JA. Low levels of hydrogen sulfide in the blood of diabetes patients and streptozotocin-treated rats causes vascular inflammation? Antioxid Redox Signal 2010;12(11):1333–7. [PubMed: 20092409]

[3]. Jain SK, Huning L, Micinski D. Hydrogen sulfide upregulates glutamate-cysteine ligase catalytic subunit, glutamate-cysteine ligase modifier subunit, and glutathione and inhibits interleukin-1beta secretion in monocytes exposed to high glucose levels. Metab Syndr Relat Disord 2014;12(5):299–302. [PubMed: 24665821]

[4]. Jain SK, Kahlon G, Bass P, Levine SN, Warden C. Can L-Cysteine and Vitamin D Rescue Vitamin D and Vitamin D Binding Protein Levels in Blood Plasma of African American Type 2 Diabetic Patients? Antioxid Redox Signal 2015;23(8):688–93. [PubMed: 25816831]

[5]. Jain SK, Kahlon G, Morehead L, Lieblong B, Stapleton T, Hoeldtke R, Bass PF, 3rd, Levine SN. The effect of sleep apnea and insomnia on blood levels of leptin, insulin resistance, IP-10, and hydrogen sulfide in type 2 diabetic patients. Metab Syndr Relat Disord 2012;10(5):331–6. [PubMed: 22746298]

[6]. Jain SK, Kanikarla-Marie P, Warden C, Micinski D. L-cysteine supplementation upregulates glutathione (GSH) and vitamin D binding protein (VDBP) in hepatocytes cultured in high glucose and in vivo in liver, and increases blood levels of GSH, VDBP, and 25-hydroxy-vitamin D in Zucker diabetic fatty rats. Mol Nutr Food Res 2016;60(5):1090–8. [PubMed: 26778482]

[7]. Jain SK, Micinski D. Vitamin D upregulates glutamate cysteine ligase and glutathione reductase, and GSH formation, and decreases ROS and MCP-1 and IL-8 secretion in high-glucose exposed U937 monocytes. Biochem Biophys Res Commun 2013;437(1):7–11. [PubMed: 23770363]

[8]. Jain SK, Micinski D, Lieblong BJ, Stapleton T. Relationship between hydrogen sulfide levels and HDL-cholesterol, adiponectin, and potassium levels in the blood of healthy subjects. Atherosclerosis 2012;225(1):242–5. [PubMed: 22989474]

[9]. Manna P, Gungor N, McVie R, Jain SK. Decreased cystathionine-gamma-lyase (CSE) activity in livers of type 1 diabetic rats and peripheral blood mononuclear cells (PBMC) of type 1 diabetic patients. J Biol Chem 2014;289(17):11767–78. [PubMed: 24610811]

[10]. Manna P, Jain SK. Vitamin D up-regulates glucose transporter 4 (GLUT4) translocation and glucose utilization mediated by cystathionine-gamma-lyase (CSE) activation and H2S formation in 3T3L1 adipocytes. J Biol Chem 2012;287(50):42324–32. [PubMed: 23074218]

[11]. Manna P, Jain SK. PIP3 but not PIP2 increases GLUT4 surface expression and glucose metabolism mediated by AKT/PKCzeta/lambda phosphorylation in 3T3L1 adipocytes. Mol Cell Biochem 2013;381(1–2):291–9. [PubMed: 23749168]

[12]. Manna P, Jain SK. L-cysteine and hydrogen sulfide increase PIP3 and AMPK/PPARgamma expression and decrease ROS and vascular inflammation markers in high glucose treated human U937 monocytes. J Cell Biochem 2013;114(10):2334–45. [PubMed: 23733596]

[13]. Sekhar RV, McKay SV, Patel SG, Guthikonda AP, Reddy VT, Balasubramanyam A, Jahoor F. Glutathione synthesis is diminished in patients with uncontrolled diabetes and restored by dietary supplementation with cysteine and glycine. Diabetes Care 2011;34(1):162–7. [PubMed: 20929994]

[14]. Rey FE, Gonzalez MD, Cheng J, Wu M, Ahern PP, Gordon JI. Metabolic niche of a prominent sulfate-reducing human gut bacterium. Proc Natl Acad Sci U S A 2013;110(33):13582–7. [PubMed: 23898195]

[15]. Bianchini F, Vainio H. Allium vegetables and organosulfur compounds: do they help prevent cancer? Environ Health Perspect 2001;109(9):893–902. [PubMed: 11673117]

[16]. Szabo C Hydrogen sulphide and its therapeutic potential. Nat Rev Drug Discov 2007;6(11):917–35. [PubMed: 17948022]

[17]. Li L, Rose P, Moore PK. Hydrogen sulfide and cell signaling. Annu Rev Pharmacol Toxicol 2011;51:169–87. [PubMed: 21210746]

[18]. Liu YH, Lu M, Hu LF, Wong PT, Webb GD, Bian JS. Hydrogen sulfide in the mammalian cardiovascular system. Antioxid Redox Signal 2012;17(1):141–85. [PubMed: 22304473]

[19]. Predmore BL, Lefer DJ, Gojon G. Hydrogen sulfide in biochemistry and medicine. Antioxid Redox Signal 2012;17(1):119–40. [PubMed: 22432697]

[20]. Tsai CY, Peh MT, Feng W, Dymock BW, Moore PK. Hydrogen sulfide promotes adipogenesis in 3T3L1 cells. PLoS One 2015;10(3):e0119511. [PubMed: 25822632]

[21]. Achari AE, Jain SK. L-Cysteine supplementation increases adiponectin synthesis and secretion, and GLUT4 and glucose utilization by upregulating disulfide bond A-like protein expression mediated by MCP-1 inhibition in 3T3-L1 adipocytes exposed to high glucose. Mol Cell Biochem 2016;414(1–2):105–13. [PubMed: 26897632]

[22]. Kanikarla-Marie P, Jain SK. L-Cysteine supplementation reduces high-glucose and ketone-induced adhesion of monocytes to endothelial cells by inhibiting ROS. Mol Cell Biochem 2014;391(1–2):251–6. [PubMed: 24627243]

[23]. Whiteman M, Gooding KM, Whatmore JL, Ball CI, Mawson D, Skinner K, Tooke JE, Shore AC. Adiposity is a major determinant of plasma levels of the novel vasodilator hydrogen sulphide. Diabetologia 2010;53(8):1722–6. [PubMed: 20414636]

[24]. Geng B, Cai B, Liao F, Zheng Y, Zeng Q, Fan X, Gong Y, Yang J, Cui QH, Tang C and others. Increase or decrease hydrogen sulfide exert opposite lipolysis, but reduce global insulin resistance in high fatty diet induced obese mice. PLoS One 2013;8(9):e73892. [PubMed: 24058499]

[25]. Padiya R, Khatua TN, Bagul PK, Kuncha M, Banerjee SK. Garlic improves insulin sensitivity and associated metabolic syndromes in fructose fed rats. Nutr Metab (Lond) 2011;8:53. [PubMed: 21794123]

[26]. Abe K, Kimura H. The possible role of hydrogen sulfide as an endogenous neuromodulator. J Neurosci 1996;16(3):1066–71. [PubMed: 8558235]

[27]. Nagai Y, Tsugane M, Oka J, Kimura H. Hydrogen sulfide induces calcium waves in astrocytes. FASEB J 2004;18(3):557–9. [PubMed: 14734631]

[28]. Nedachi T, Kanzaki M. Regulation of glucose transporters by insulin and extracellular glucose in C2C12 myotubes. Am J Physiol Endocrinol Metab 2006;291(4):E817–28. [PubMed: 16735448]

[29]. Candiloros H, Muller S, Zeghari N, Donner M, Drouin P, Ziegler O. Decreased erythrocyte membrane fluidity in poorly controlled IDDM. Influence of ketone bodies. Diabetes Care 1995;18(4):549–51. [PubMed: 7497868]

[30]. Jin S, Pu SX, Hou CL, Ma FF, Li N, Li XH, Tan B, Tao BB, Wang MJ, Zhu YC. Cardiac H2S Generation Is Reduced in Ageing Diabetic Mice. Oxid Med Cell Longev 2015;2015:758358. [PubMed: 26078817]

[31]. Lin VS, Lippert AR, Chang CJ. Cell-trappable fluorescent probes for endogenous hydrogen sulfide signaling and imaging H2O2-dependent H2S production. Proc Natl Acad Sci U S A 2013;110(18):7131–5. [PubMed: 23589874]

[32]. Rubinstein R, Genaro AM, Motta A, Cremaschi G, Wald MR. Impaired immune responses in streptozotocin-induced type I diabetes in mice. Involvement of high glucose. Clin Exp Immunol 2008;154(2):235–46. [PubMed: 18778365]

[33]. Barja G Mitochondrial oxygen radical generation and leak: sites of production in states 4 and 3, organ specificity, and relation to aging and longevity. J Bioenerg Biomembr 1999;31(4):347–66. [PubMed: 10665525]

[34]. Borras C, Gambini J, Gomez-Cabrera MC, Sastre J, Pallardo FV, Mann GE, Vina J. 17beta-oestradiol up-regulates longevity-related, antioxidant enzyme expression via the ERK1 and ERK2[MAPK]/NFkappaB cascade. Aging Cell 2005;4(3):113–8. [PubMed: 15924567]

[35]. Jung DW, Ha HH, Zheng X, Chang YT, Williams DR. Novel use of fluorescent glucose analogues to identify a new class of triazine-based insulin mimetics possessing useful secondary effects. Mol Biosyst 2011;7(2):346–58. [PubMed: 20927436]

[36]. Schmittgen TD, Livak KJ. Analyzing real-time PCR data by the comparative C(T) method. Nat Protoc 2008;3(6):1101–8. [PubMed: 18546601]

[37]. Pfeiffer CM, Huff DL, Gunter EW. Rapid and accurate HPLC assay for plasma total homocysteine and cysteine in a clinical laboratory setting. Clin Chem 1999;45(2):290–2. [PubMed: 9931056]

[38]. Ilgu H, Jeckelmann JM, Gapsys V, Ucurum Z, de Groot BL, Fotiadis D. Insights into the molecular basis for substrate binding and specificity of the wild-type L-arginine/agmatine antiporter AdiC. Proc Natl Acad Sci U S A 2016;113(37):10358–63. [PubMed: 27582465]

[39]. Deng D, Sun P, Yan C, Ke M, Jiang X, Xiong L, Ren W, Hirata K, Yamamoto M, Fan S and others. Molecular basis of ligand recognition and transport by glucose transporters. Nature 2015;526(7573):391–6. [PubMed: 26176916]

[40]. Hresko RC, Kraft TE, Quigley A, Carpenter EP, Hruz PW. Mammalian Glucose Transporter Activity Is Dependent upon Anionic and Conical Phospholipids. J Biol Chem 2016;291(33): 17271–82. [PubMed: 27302065]

[41]. Altschul SF, Madden TL, Schaffer AA, Zhang J, Zhang Z, Miller W, Lipman DJ. Gapped BLAST and PSI-BLAST: a new generation of protein database search programs. Nucleic Acids Res 1997;25(17):3389–402. [PubMed: 9254694]

[42]. Remmert M, Biegert A, Hauser A, Soding J. HHblits: lightning-fast iterative protein sequence searching by HMM-HMM alignment. Nat Methods 2011;9(2):173–5. [PubMed: 22198341]

[43]. Benkert P, Biasini M, Schwede T. Toward the estimation of the absolute quality of individual protein structure models. Bioinformatics 2011;27(3):343–50. [PubMed: 21134891]

[44]. Arnold K, Bordoli L, Kopp J, Schwede T. The SWISS-MODEL workspace: a web-based environment for protein structure homology modelling. Bioinformatics 2006;22(2):195–201. [PubMed: 16301204]

[45]. Biasini M, Bienert S, Waterhouse A, Arnold K, Studer G, Schmidt T, Kiefer F, Gallo Cassarino T, Bertoni M, Bordoli L and others. SWISS-MODEL: modelling protein tertiary and quaternary structure using evolutionary information. Nucleic Acids Res 2014;42(Web Server issue):W252–8. [PubMed: 24782522]

[46]. Lewerenz J, Hewett SJ, Huang Y, Lambros M, Gout PW, Kalivas PW, Massie A, Smolders I, Methner A, Pergande M and others. The cystine/glutamate antiporter system x(c)(−) in health and disease: from molecular mechanisms to novel therapeutic opportunities. Antioxid Redox Signal 2013;18(5):522–55. [PubMed: 22667998]

[47]. Kabil O, Vitvitsky V, Xie P, Banerjee R. The quantitative significance of the transsulfuration enzymes for H2S production in murine tissues. Antioxid Redox Signal 2011;15(2):363–72. [PubMed: 21254839]

[48]. Rains JL, Jain SK. Oxidative stress, insulin signaling, and diabetes. Free Radic Biol Med 2011;50(5):567–75. [PubMed: 21163346]

[49]. Dalle-Donne I, Rossi R, Giustarini D, Colombo R, Milzani A. S-glutathionylation in protein redox regulation. Free Radic Biol Med 2007;43(6):883–98. [PubMed: 17697933]

[50]. Niwa T Protein glutathionylation and oxidative stress. J Chromatogr B Analyt Technol Biomed Life Sci 2007;855(1):59–65.

[51]. Muniz P, Valls V, Perez-Broseta C, Iradi A, Climent JV, Oliva MR, Saez GT. The role of 8-hydroxy-2'-deoxyguanosine in rifamycin-induced DNA damage. Free Radic Biol Med 1995;18(4):747–55. [PubMed: 7750799]

[52]. Chen Y, Johansson E, Fan Y, Shertzer HG, Vasiliou V, Nebert DW, Dalton TP. Early onset senescence occurs when fibroblasts lack the glutamate-cysteine ligase modifier subunit. Free Radic Biol Med 2009;47(4):410–8. [PubMed: 19427898]

[53]. Ballatori N, Krance SM, Notenboom S, Shi S, Tieu K, Hammond CL. Glutathione dysregulation and the etiology and progression of human diseases. Biol Chem 2009;390(3):191–214. [PubMed: 19166318]

[54]. Harvey CJ, Thimmulappa RK, Singh A, Blake DJ, Ling G, Wakabayashi N, Fujii J, Myers A, Biswal S. Nrf2-regulated glutathione recycling independent of biosynthesis is critical for cell survival during oxidative stress. Free Radic Biol Med 2009;46(4):443–53. [PubMed: 19028565]

[55]. Xie L, Gu Y, Wen M, Zhao S, Wang W, Ma Y, Meng G, Han Y, Wang Y, Liu G and others. Hydrogen Sulfide Induces Keap1 S-sulfhydration and Suppresses Diabetes- Accelerated Atherosclerosis via Nrf2 Activation. Diabetes 2016;65(10):3171–84. [PubMed: 27335232]

[56]. Yang G, Zhao K, Ju Y, Mani S, Cao Q, Puukila S, Khaper N, Wu L, Wang R. Hydrogen sulfide protects against cellular senescence via S-sulfhydration of Keap1 and activation of Nrf2. Antioxid Redox Signal 2013;18(15):1906–19. [PubMed: 23176571]

[57]. Itoh K, Mimura J, Yamamoto M. Discovery of the negative regulator of Nrf2, Keap1: a historical overview. Antioxid Redox Signal 2010;13(11):1665–78. [PubMed: 20446768]

[58]. Cramer SL, Saha A, Liu J, Tadi S, Tiziani S, Yan W, Triplett K, Lamb C, Alters SE, Rowlinson S and others. Systemic depletion of L-cyst(e)ine with cyst(e)inase increases reactive oxygen species and suppresses tumor growth. Nat Med 2016.

[59]. Wang R Physiological implications of hydrogen sulfide: a whiff exploration that blossomed. Physiol Rev 2012;92(2):791–896. [PubMed: 22535897]

[60]. Lushchak VI. Glutathione homeostasis and functions: potential targets for medical interventions. J Amino Acids 2012;2012:736837. [PubMed: 22500213]

[61]. Nordberg J, Arner ES. Reactive oxygen species, antioxidants, and the mammalian thioredoxin system. Free Radic Biol Med 2001;31(11):1287–312. [PubMed: 11728801]

[62]. Lee ZW, Low YL, Huang S, Wang T, Deng LW. The cystathionine gamma- lyase/hydrogen sulfide system maintains cellular glutathione status. Biochem J 2014;460(3):425–35. [PubMed: 24707893]

[63]. Watson RT, Kanzaki M, Pessin JE. Regulated membrane trafficking of the insulin- responsive glucose transporter 4 in adipocytes. Endocr Rev 2004;25(2):177–204. [PubMed: 15082519]

[64]. Huang S, Czech MP. The GLUT4 glucose transporter. Cell Metab 2007;5(4):237–52. [PubMed: 17403369]

[65]. Yamamoto J, Sato W, Kosugi T, Yamamoto T, Kimura T, Taniguchi S, Kojima H, Maruyama S, Imai E, Matsuo S and others. Distribution of hydrogen sulfide (H(2)S)- producing enzymes and the roles of the H(2)S donor sodium hydrosulfide in diabetic nephropathy. Clin Exp Nephrol 2013;17(1):32–40. [PubMed: 22872231]

[66]. Yang G, Wu L, Jiang B, Yang W, Qi J, Cao K, Meng Q, Mustafa AK, Mu W, Zhang S and others. H2S as a physiologic vasorelaxant: hypertension in mice with deletion of cystathionine gamma-lyase. Science 2008;322(5901):587–90. [PubMed: 18948540]

Highlights

- H_2S upregulates GCL, GSS, and GR, increases GSH, and decreases ROS levels
- H_2S stimulates GSH-dependent antioxidant defense in myotubes
- H_2S regulates cysteine homeostasis through LC transporter
- H_2S enhances GLUT4 and glucose uptake
- The CSE/H_2S system maintains glutathione and glucose homeostasis in myotubes

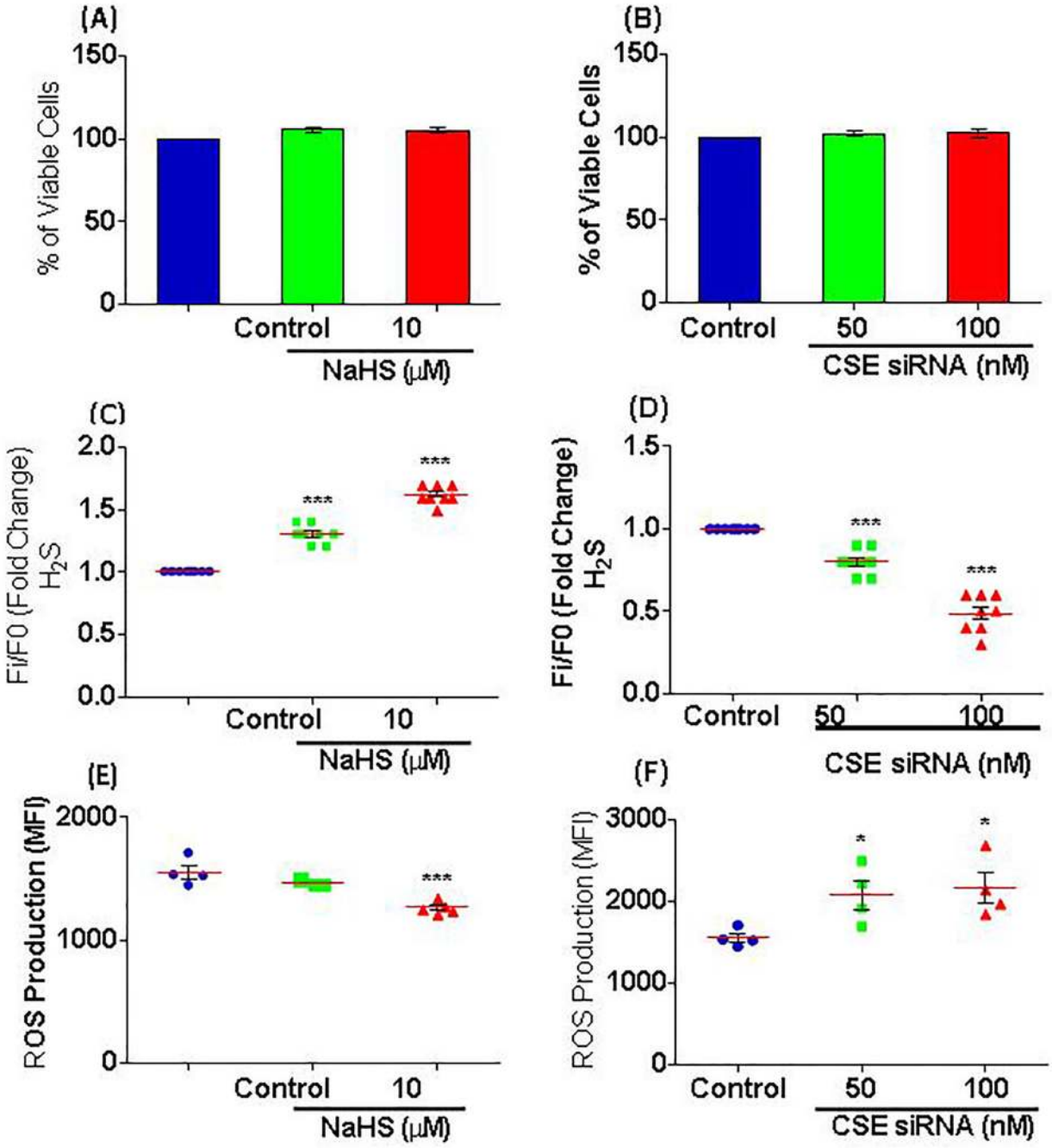

Figure 1.

Effect of NaHS [0, 10 or 20 μM] treatment and CSE siRNA transfection [50 or 100 nM] on the cell viability **(A, B)**, levels of intracellular H_2S (**C, D**), and ROS production **(E, F)** in C_2C_{12} mouse myoblasts. Control siRNA is a scrambled nonspecific RNA duplex with no sequence homology with any of the genes. Data are expressed as mean ± SEM (n ≥4). * $p <$ 0.05,** $p < 0.01$, *** $p< 0.001$ vs. control.

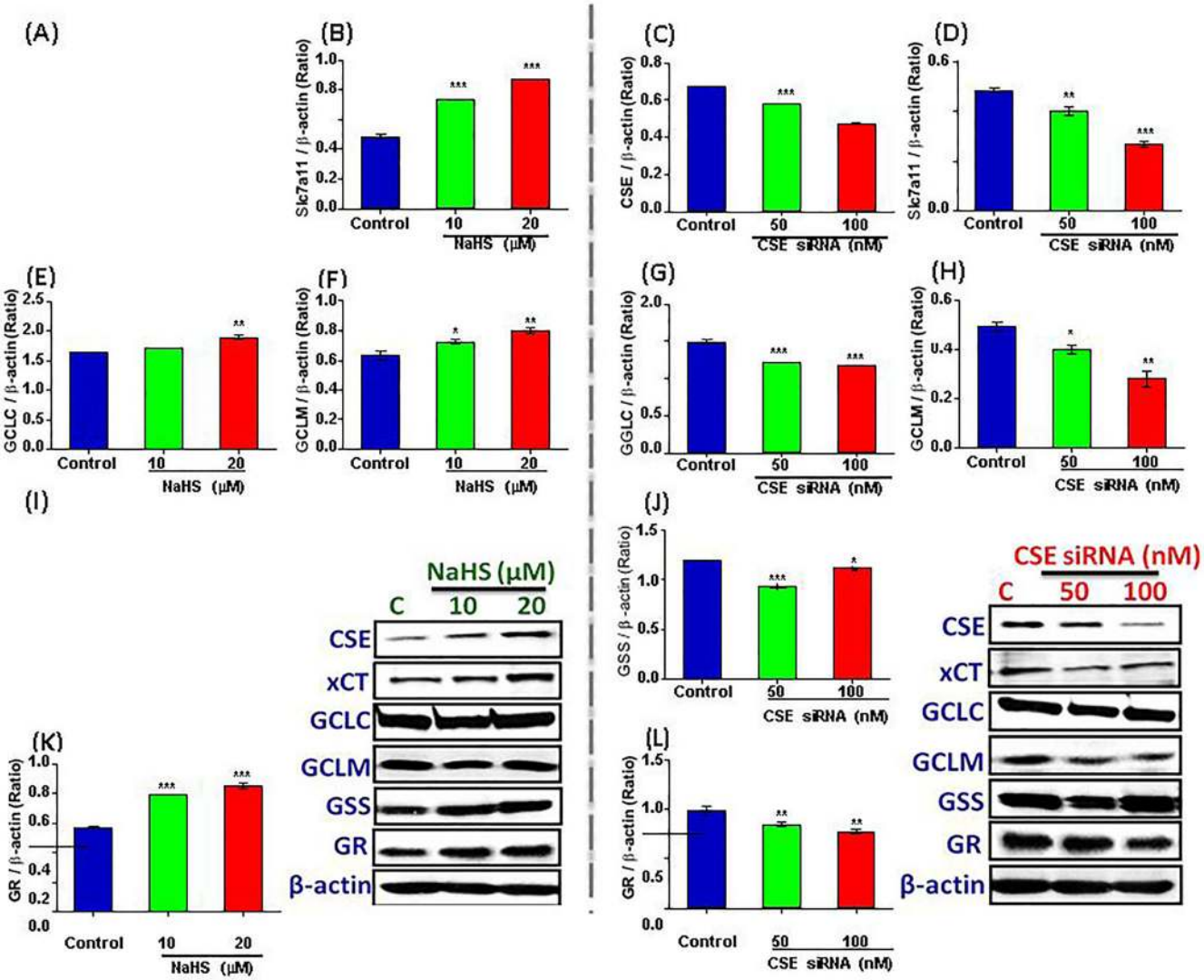

Figure 2.

Effect of NaHS [0, 10 or 20 μM] treatment **(left panel)** and CSE siRNA transfection [50 or 100 nM] (**right panel)** on the expression levels of protein CSE (**A, C**); xCT/Slc7A11**(B, D)**; GCLC **(E, G)**; GCLM **(F, H)**; GSS **(I, J)**; and GR **(K, L)** in C_2C_{12} mouse myoblasts. Data are expressed as mean ± SEM (n = 4). * $p < 0.05$,** $p < 0.01$, *** $p < 0.001$ vs. control.

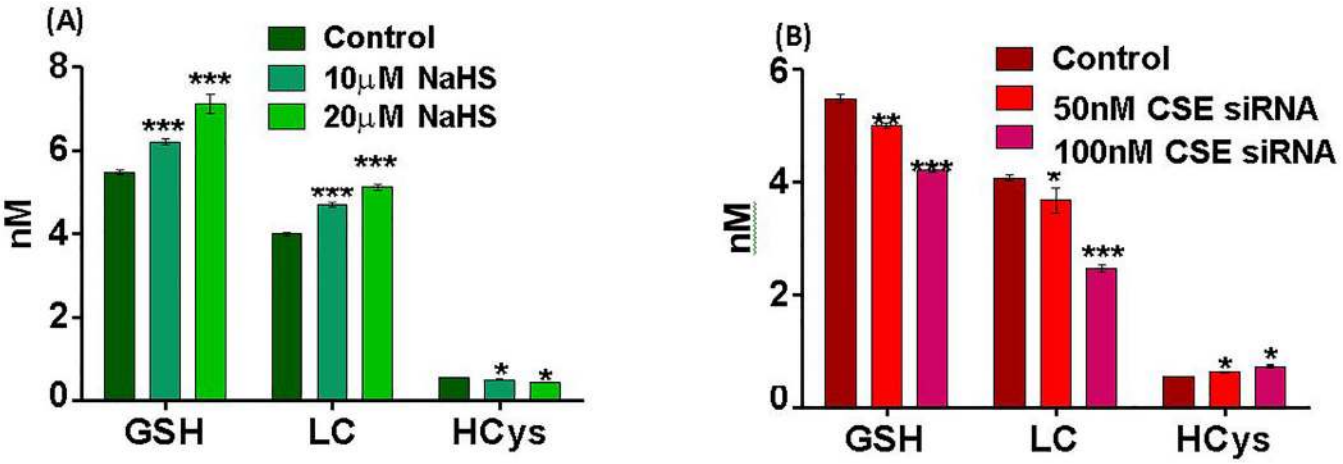

Figure 3.

Effect of NaHS [0, 10 or 20 μM] treatment **(A)** and CSE siRNA transfection [50 or 100 nM] **(B)** on the levels of glutathione (GSH), L-Cysteine (LC), and homocysteine (HCys) in C_2C_{12} mouse myoblasts. Data are expressed as mean ± SEM (n = 4). * $p < 0.05$,** $p < 0.01$, *** $p < 0.001$ vs. control.

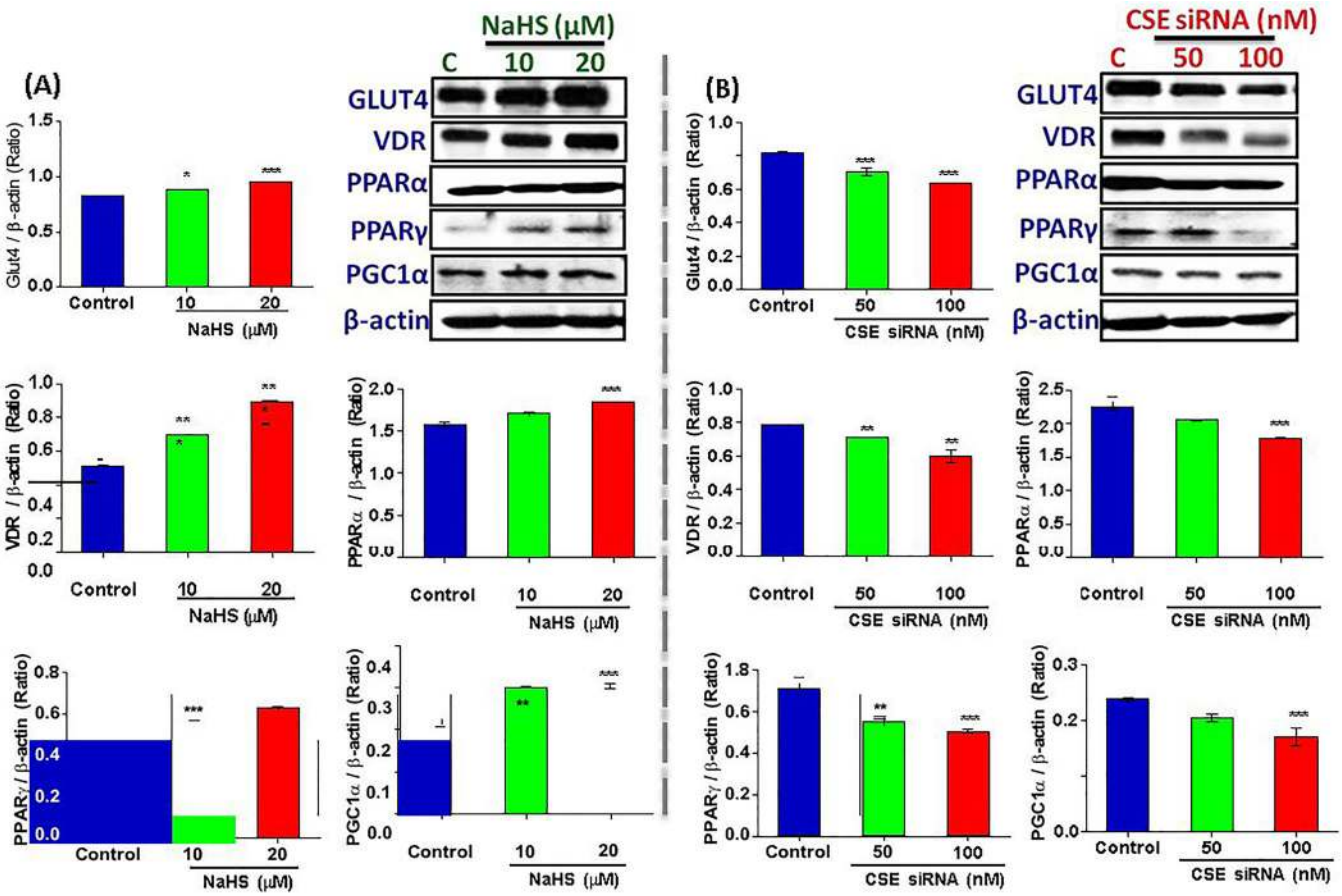

Figure 4.

Effect of NaHS [0, 10 or 20 μM] treatment **(left panel)** and CSE siRNA transfection [50 or 100 nM] (**right panel)** on the expression levels of protein GLUT4/Slc2a4 (**A, B**); VDR **(C, E)**; PPARα **(D, F)**; PPARγ **(G, I)**; and PGC1α **(H, J)** in C_2C_{12} mouse myoblasts. Data are expressed as mean ± SEM (n = 4). * $p < 0.05$,** $p < 0.01$, *** $p < 0.001$ vs. control.

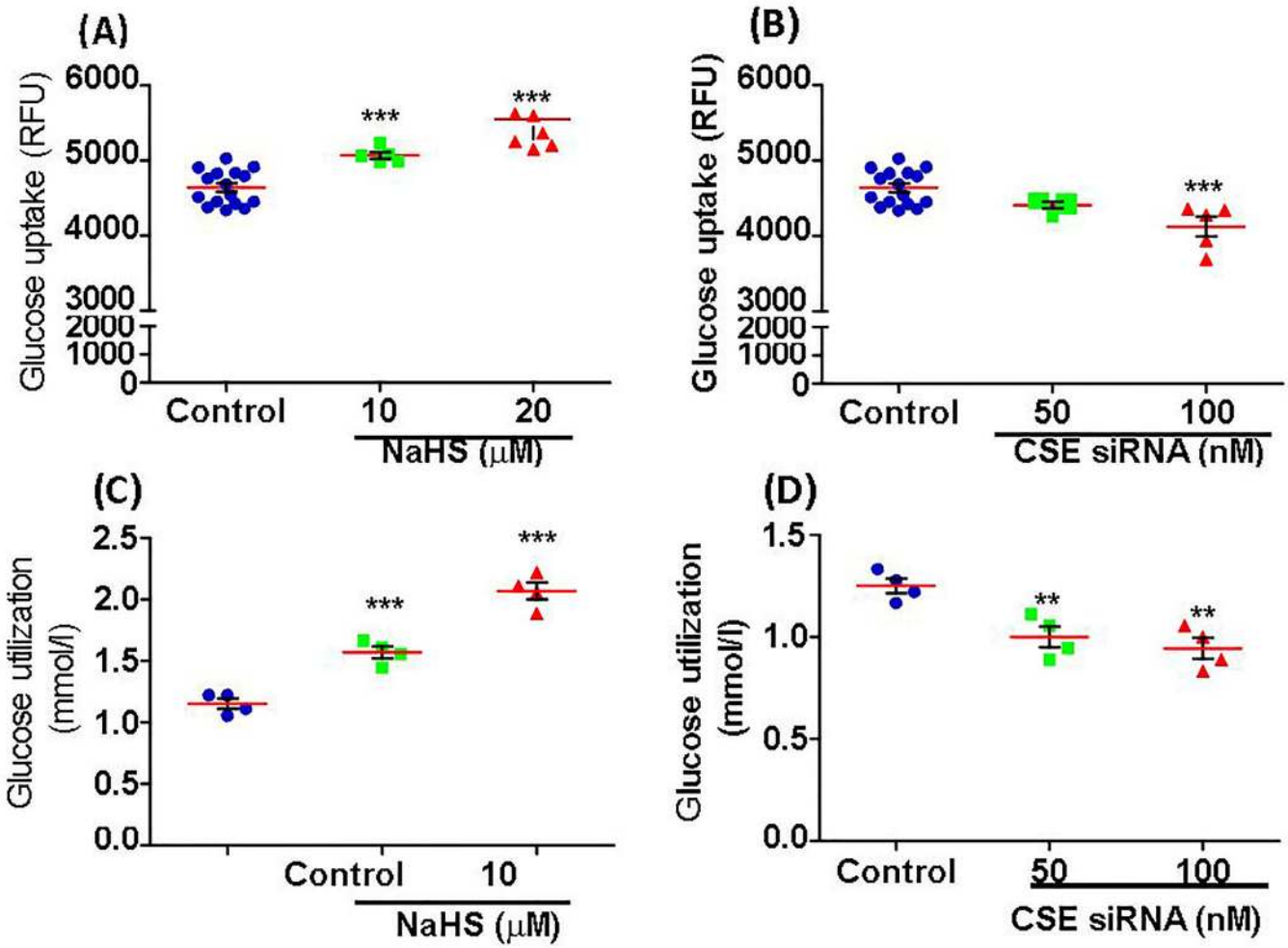

Figure 5.

Effect of NaHS [0, 10 or 20 μM] treatment **(left panel)** and CSE siRNA transfection [50 or 100 nM] (**right panel)** on glucose uptake (**A**) and utilization **(B)** in C_2C_{12} mouse myoblasts. Glucose uptake was measured using fluorescent 6-NBDG (analogue of 2- dexoyglucose), a fluorescent probe. The glucose utilization level was determined by subtracting glucose values at the end of the experiments (leftover glucose) from the 0 h glucose level. A glucose meter was used for the glucose utilization assay. Data are expressed as mean ± SEM (n ≥4). * $p < 0.05$,** $p < 0.01$, *** $p< 0.001$ vs. control.

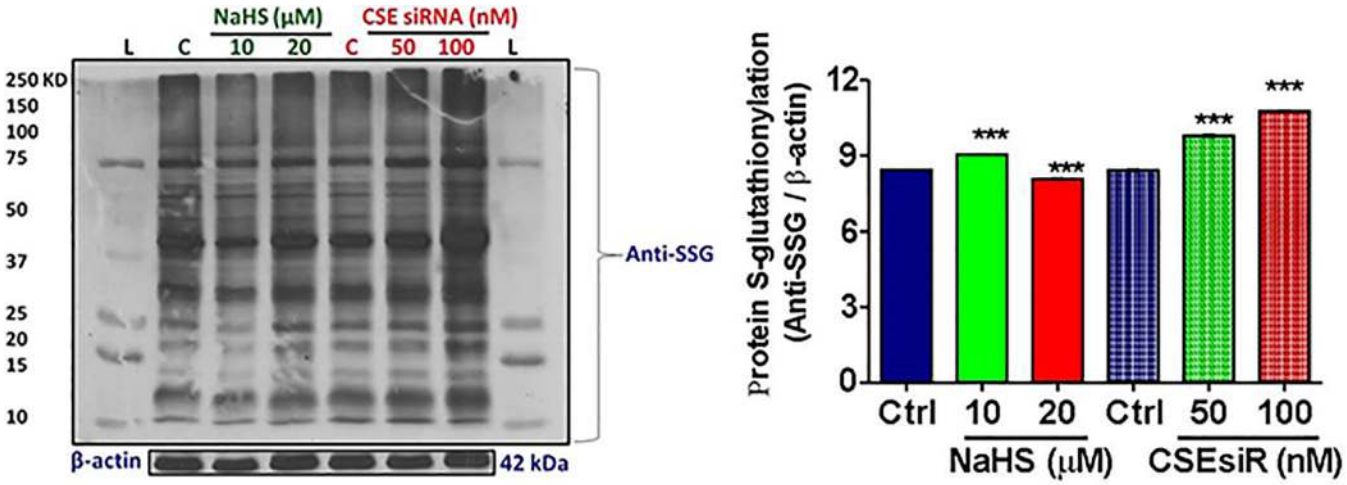

Figure 6.

Effect of NaHS [0, 10 or 20 μM] treatment and CSE siRNA transfection [50 or 100 nM] on total protein S-glutathionylation in C_2C_{12} mouse myoblasts. Total protein S-glutathionylation was quantified with an anti-GSH antibody and normalized with β-actin under non-denaturing conditions. Data are expressed as mean ± SEM (n = 4). * $p < 0.05$,** $p < 0.01$, *** $p < 0.001$ vs. control.

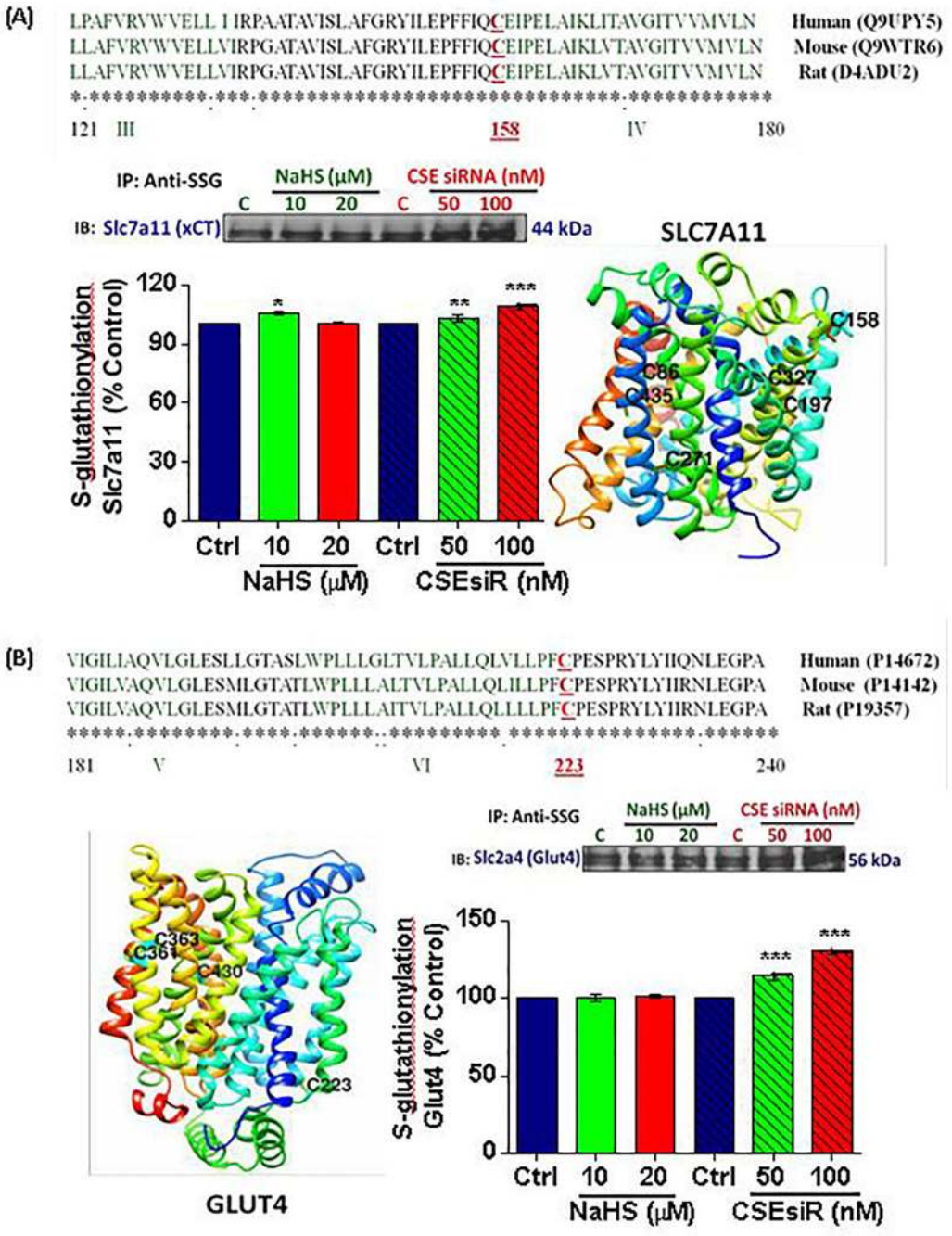

Figure 7.

Effect of NaHS [0, 10 or 20 μM] treatment and CSE siRNA transfection [50 or 100 nM] on Slc7a11/xCT **(A)** and Slc2a4/Glut4 protein S-glutathionylation **(B)** in C_2C_{12} mouse myoblasts. Sequence alignments and molecular models are provided, with all six conserved cysteines (Slc7a11, **A**) and all four conserved cysteines (Slc2a4, **B**) indicated, respectively. The model was built based on the structures of *Escherichia coli* (Protein Data Bank code 5J4I) and human GLUT3 (4ZW9), respectively. In the amino acid sequences of human, mouse, and rat Slc7a11 and Slc2a4, the positions of the cysteine[158] in Slc7a11/xCT and

cysteine^{223} in Slc2a4/Glut4 were marked. Roman numerals denote the transmembrane domain of these proteins respectively (III and IV in Slc7a11, and V and VI in Slc2a4). SWISS-MODEL workspace and Uniprot were used to generate models and sequence alignments. For immunoprecipitation assays, antigen-antibody complexes (anti-GSH) were pulled down by incubation with protein A/G agarose, and Western blots with anti-xCT and anti-GLUT4, and quantified. Detected bands were normalized with control and expressed as % control. Data are expressed as mean ± SEM (n = 4). * $p < 0.05$,** $p < 0.01$, *** $p < 0.001$ vs. control.

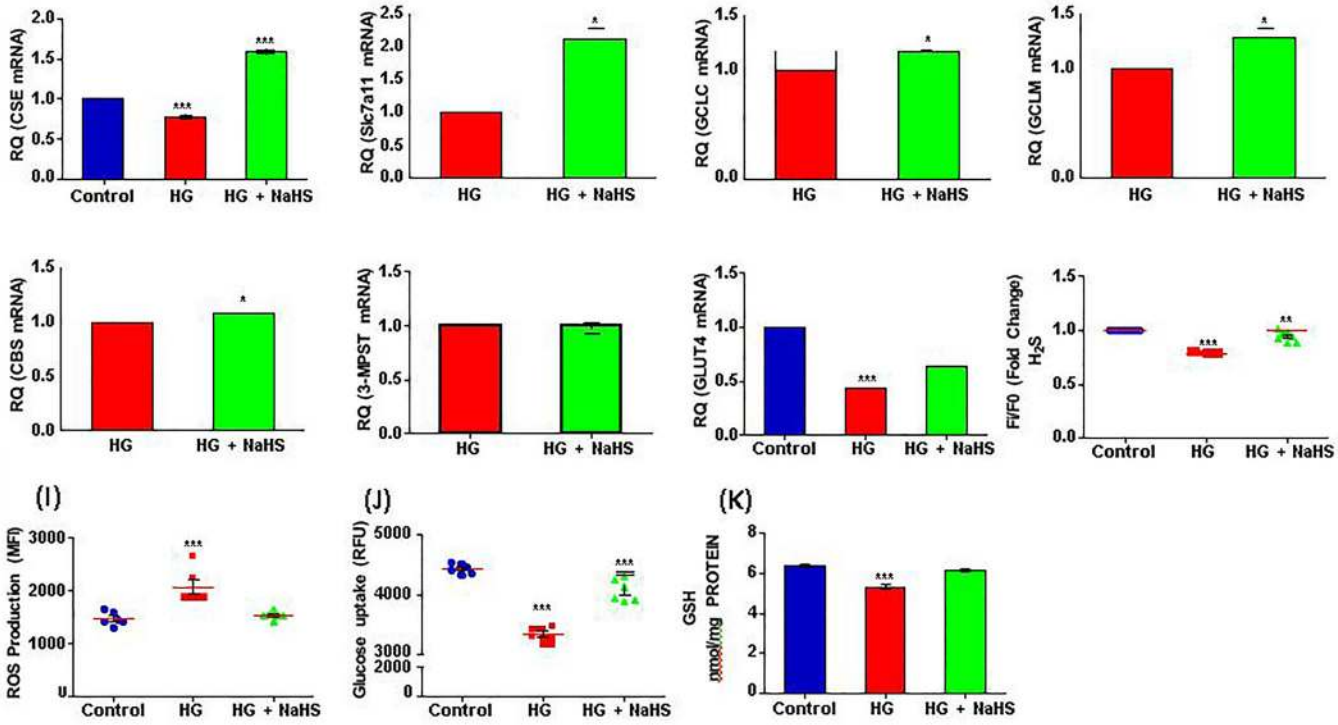

Figure 8.

Effect of NaHS [20 μM] treatment on high glucose (25 mM) exposed myotubes on the expression levels of mRNA: CSE (**A**); xCT/Slc7A11**(B)**; GCLC **(C)**; GCLM **(D)**; CBS **(E)**; 3- MPST **(F)**; GLUT4 (**G**) and, H_2S **(H)**; ROS **(I)**; glucose uptake **(J)** and GSH **(K)** levels in C_2C_{12} mouse myoblasts. Data are expressed as mean ± SEM (n ≥4). * $p < 0.05$,** $p < 0.01$, *** $p< 0.001$ vs. control.

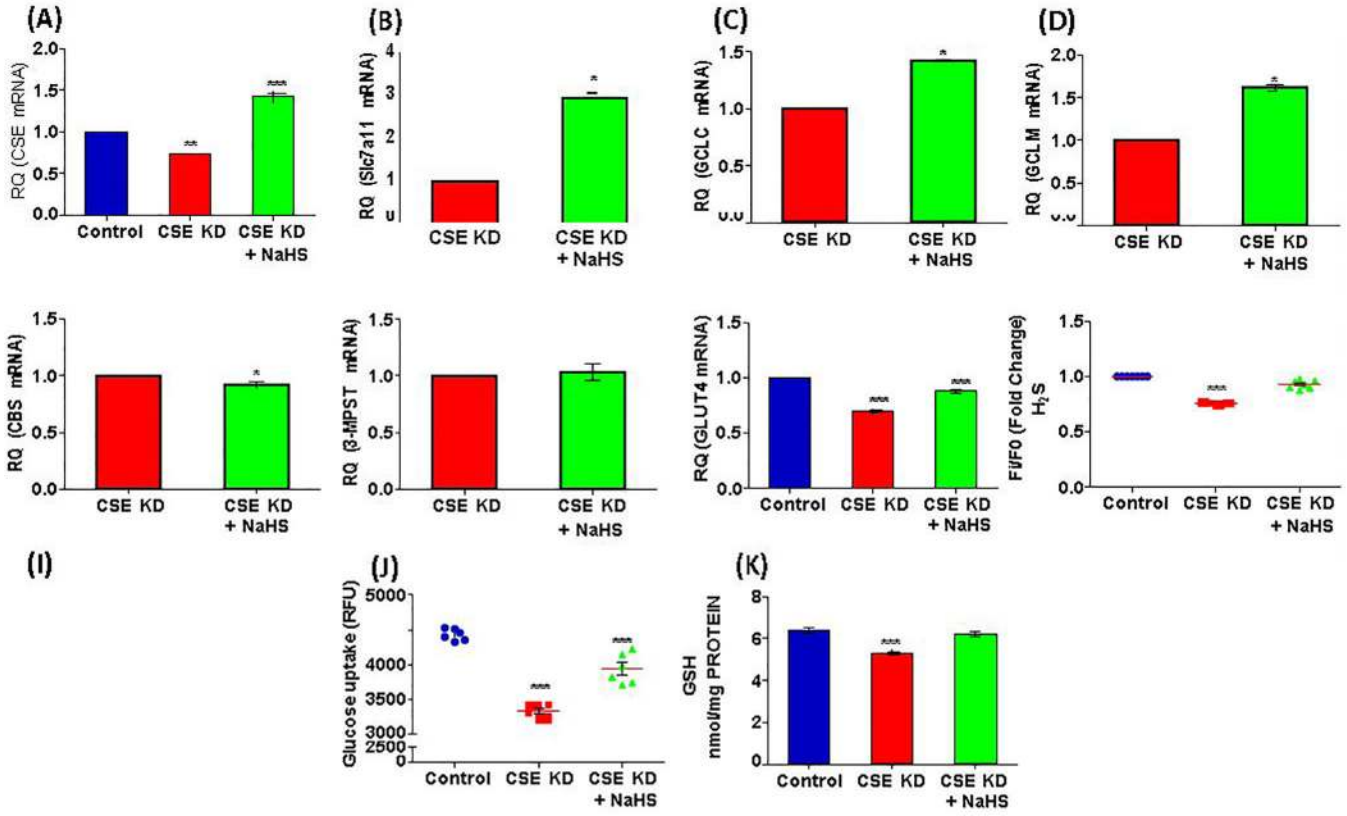

Figure 9.

Effect of NaHS [20 μM] treatment on CSE deficient myotubes [100 nM siRNA] on the expression levels of mRNA: CSE (**A**); xCT/Slc7A11**(B)**; GCLC **(C)**; GCLM **(D)**; CBS **(E)**; 3- MPST **(F)**; GLUT4 (**G**) and, H_2S **(H)**; ROS **(I)**; glucose uptake **(J)** and GSH **(K)** levels in C_2C_{12} mouse myoblasts. Data are expressed as mean ± SEM (n ≥4). * $p < 0.05$,** $p < 0.01$, *** $p < 0.001$ vs. control.

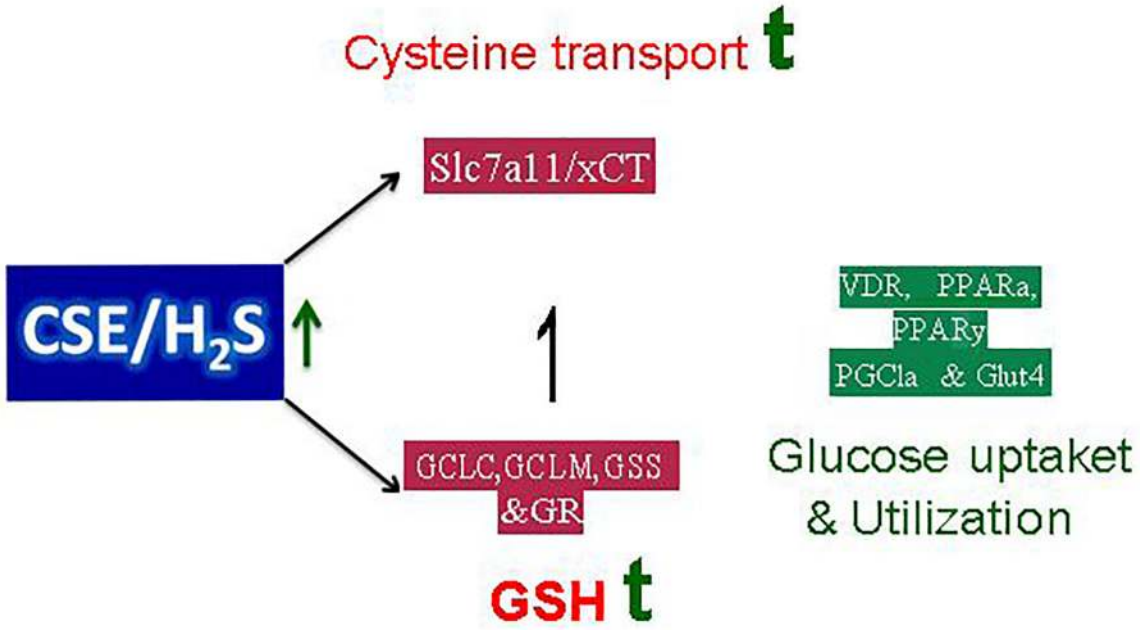

Figure 10.
Schematic diagram of proposed mechanism by which CSE/H_2S system maintains cellular glutathione and glucose homeostasis in C_2C_{12} mouse myotubes.